Inorg. Chem. **2004**, *43*, 7994–8004

Chiral Induction in Self-Assembled Helicates: CHIRAGEN Type Ligands with Ferrocene Bridging Units

Boris Quinodoz,[†] Gaël Labat,[‡] Helen Stoeckli-Evans,[‡,§] and Alex von Zelewsky*[,†]

Department of Chemistry, University of Fribourg, Pérolles, CH-1700 Fribourg, Switzerland, and Institute of Chemistry, University of Neuchâtel, Av. Bellevaux 51, CH-2007 Neuchâtel, Switzerland

Received January 20, 2004

The aim of this work was the preparation of enantiomerically pure bis(pinene–bipyridine) ligands containing the ferrocenyl moiety. Several such ligands (**1**–**3**) were synthesized and completely characterized. These molecules can be diastereoselectively deprotonated at the acidic methylene group of the pinene moiety using a strong and sterically hindered base such as LDA. Subsequent reaction of the formed anion with alkyl halides yield the family of C_2-symmetric enantiopure compounds (**1a**–**c**). Copper(I), silver(I), or zinc(II) complexes with several ligands (**C1**–**C8**) were prepared and structurally characterized in the solid state and in solution. Self-assembled helical species are formed in several cases. It became evident that the chiral groups present in the ligand do not completely determined the helical configuration of the assemblages. Diastereoselectivity is thus not complete with this type of ligands, contrary to other, similar ligands studied before.

Introduction

The field of stereoselective synthesis of coordination compounds using chiral ligands has developed during the past decade at an increasing rate.[1−11] An important subset of coordination species where stereoselectivity is important is the field of chiral self-assembled architectures. The numerous helicates that were reported recently[2] are paradigmatic examples of such molecular structures. Among the various classes of ligands that have shown to be suitable for the construction of self-assemblages, N-heterocycles are particularly numerous. We have successfully used CHIRAGEN type ligands (Chart 1) in self-assembly reactions leading to various types of supramolecular structures with predetermined configurations.[8,12−17]

Chart 1

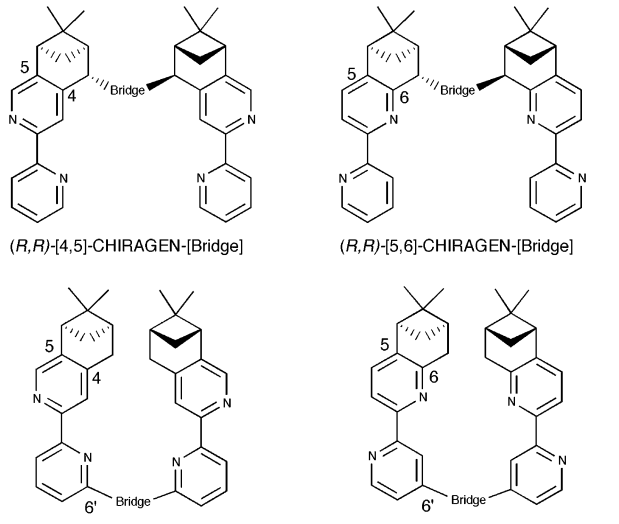

* Author to whom correspondence should be addressed. E-mail: Alexander.vonzelewsky@unifr.ch. Fax: ++41263009738. Tel.: ++412630-08732.
[†] University of Fribourg.
[‡] University of Neuchâtel.
[§] E-mail: Helen.Stoeckli-Evans@unine.ch.

(1) Constable, E. C. *Tetrahedron* **1992**, *48*, 10013.
(2) Piguet, C.; Bernadinelli, G.; Hopfgartner, G. *Chem. Rev.* **1997**, *97*, 2005.
(3) Albrecht, M. *Chem. Soc. Rev.* **1998**, *27*, 281.
(4) Albrecht, M. *Chem.—Eur. J.* **2000**, *6*, 3485.
(5) Albrecht, M. *Chem. Rev. (Washington, D.C.)* **2001**, *101*, 3457.
(6) Caulder, D. L.; Raymond, K. N. *J. Chem. Soc., Dalton Trans.* **1999**, 1185.
(7) Caulder, D. L.; Raymond, K. N. *Acc. Chem. Res.* **1999**, *32*, 975.
(8) von Zelewsky, A. *Coord. Chem. Rev.* **1999**, *190−192*, 811.
(9) Knof, U.; Von Zelewsky, A. *Angew. Chem., Int. Ed.* **1999**, *38*, 303.
(10) Fang, C.-J.; Duan, H.-M.; He, C.; Meng, Q.-J.; Liu, Y.-J.; Mei, Y.-H.; Wang, Z.-M. *Organometallics* **2001**, *20*, 2525.
(11) Ziessel, R. *Inorg. Chem.* **1998**, *37*, 4146.
(12) Mamula, O.; von Zelewsky, A.; Bernardinelli, G. *Angew. Chem., Int. Ed.* **1998**, *37*, 290.
(13) Mamula, O.; Von Zelewsky, A.; Bark, T.; Bernardinelli, G. *Angew. Chem., Int. Ed.* **1999**, *38*, 2945.
(14) Mamula, O.; Von Zelewsky, A.; Bark, T.; Stoeckli-Evans, H.; Neels, A.; Bernardinelli, G. *Chem.—Eur. J.* **2000**, *6*, 3575.
(15) Mamula, O.; Monlien, F. J.; Porquet, A.; Hopfgartner, G.; Merbach, A. E.; von Zelewsky, A. *Chem.—Eur. J.* **2001**, *7*, 533.

10.1021/ic049913a CCC: $27.50
Published on Web 11/06/2004

Chart 2

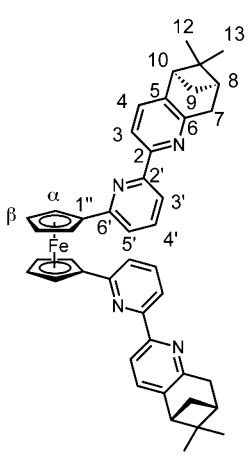

Bis-(*R,R*)-[5,6]-pinene-bipyridyl-6'-[ferrocene]

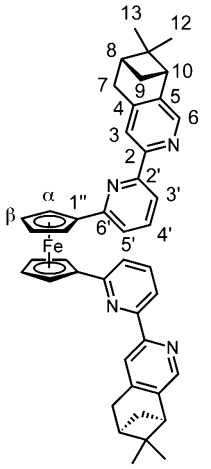

Bis-(*R,R*)-[4,5]-pinene-bipyridyl-6'-[ferrocene]

Recently other examples of stereoselective self-assembled helicates were described using a bis-bpy ligand[18] where the stereogenic element is introduced via an axially chiral BINOL moiety connecting the two bpy units.

Here we present new members of a variation of the CHIRAGEN family, where two bipyridine units are connected not through the pinene moieties but directly at the 6′ position of one of the pyridine rings (Chart 1).[17,19,20] In the present case the bridge is formed by ferrocenyl units (Chart 2).

Ligands **1**−**3** (Chart 3) are tetradentate ligands based on pinene−bipyridine moieties, which are able to form double-stranded helices when reacted with metal cations such as Cu(I), Ag(I), or Zn(II).

Moreover the presence of pinene groups should discriminate the formation of a *P* or *M* helix, respectively, thus resulting in a diastereoselective complex formation.

Ligands **1a**−**c** (Chart 3) are alkylated derivatives of bis-((*R,R*)-[5,6]pinene−bipyridyl)−6′-[ferrocene], **1**, possessing respectively methyl, benzyl, and isopropyl groups in the position 7 of the pinene. The latter series of ligands was synthesized to compare the diastereoselective induction of the pinene groups when the complexes are formed.

For the synthesis of these ligands we used homo-coupling reactions (Negishi, Suzuki) (Scheme 1). Similar synthetic methods were used by other authors for the fabrication of ferrocenyl derivatives.[21,22]

Results and Discussion

The chiral ligands **1**−**3** were obtained following two different synthetic routes (Scheme 1). Starting from the commercially available diboronic acid **A**, a Suzuki coupling using $Pd(PPh_3)_4$ or $Pd(PPh_3)_2Cl_2$ as palladium catalysts was caried out. Starting from the dilithiated ferrocene B (2:3 complex with TMEDA),[23] the products **1**−**3** are obtained via Negishi coupling. The results obtained for the couplings are reported in Table 1.

Chart 3

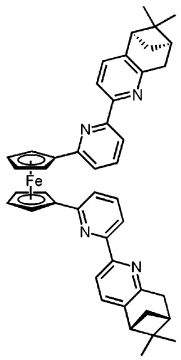

1

Bis-(*R,R*)-[5,6]-pinene-bipyridyl-6'-[ferrocene]

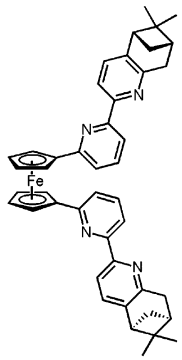

2

Bis-(*S,S*)-[5,6]-pinene-bipyridyl-6'-[ferrocene]

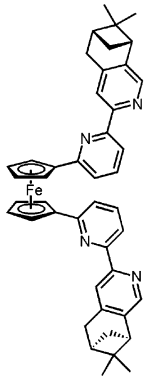

3

Bis-(*R,R*)-[4,5]-pinene-bipyridyl-6'-[ferrocene]

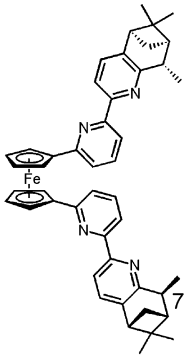

1a

Bis-(*R,R*)-7-dimethyl-[5,6]-pinene-bipyridyl-6'-[ferrocene]

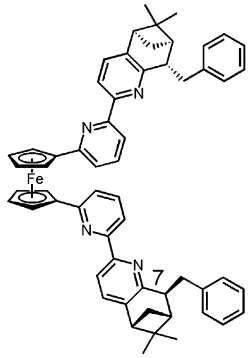

1b

Bis-(*R,R*)-7-dibenzyl-[5,6]-pinene-bipyridyl-6'-[ferrocene]

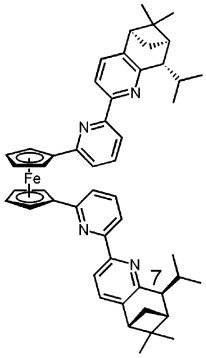

1c

Bis-(*R,R*)-7-diisopropyl-[5,6]-pinene-bipyridyl-6'-[ferrocene]

Scheme 1

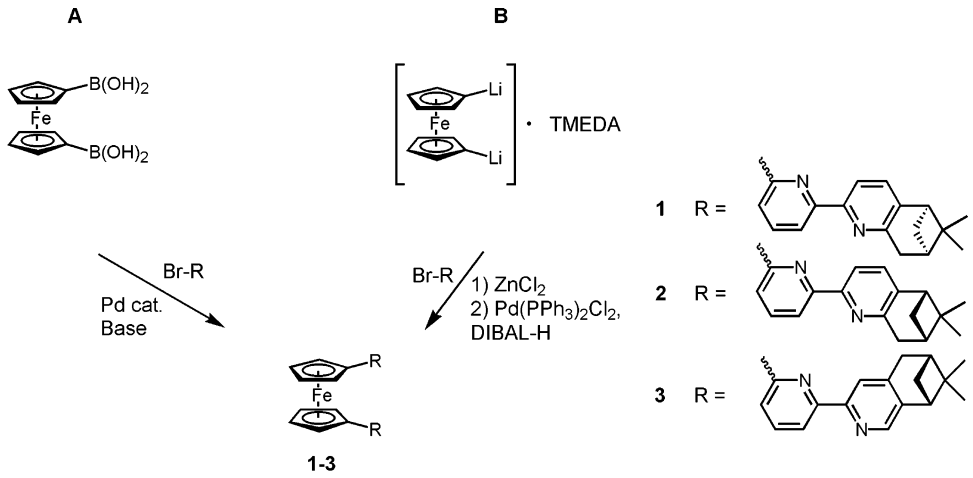

Table 1. Summary of Synthetic Procedures for Products **1**−**3**

entry	starting material	catalyst	solvent/base	product, yield (%)
1	A	$Pd(PPh_3)_4$	toluene/K_2CO_3	**1**, 25
2	B	$Pd(PPh_3)_2Cl_2$/DIBAL-H	THF	**1**, 26
3	B	$Pd(PPh_3)_2Cl_2$/DIBAL-H	THF	**2**, 18
4	A	$Pd(dppf)_2Cl_2$	DME/K_2CO_3	**3**, 7
5	B	$Pd(PPh_3)_2Cl_2$/DIBAL-H	THF	**3**, 20

The low yields obtained can be easily explained, since the dilithioferrocene−2/3TMEDA adduct is quite unstable at higher temperatures or against traces of moisture and oxygen. This behavior explains also the 15−20% pure ferrocene which is always recovered at the end of the reaction. Then, more generally, the steric hindrance generated by the coupling formation (presence of the catalyst, pinene groups) certainly diminishes the efficiency of the coupling. Monosubstituted ferrocenyl derivatives were observed to give up to 60% yield depending on the starting product and detailed conditions.

The ^{1}H NMR of the ferrocenyl derivatives **1** (**1** and **2** are enantiomers, yielding identical NMR spectra) and **3** are presented in Figure 1. These two compounds are similar in

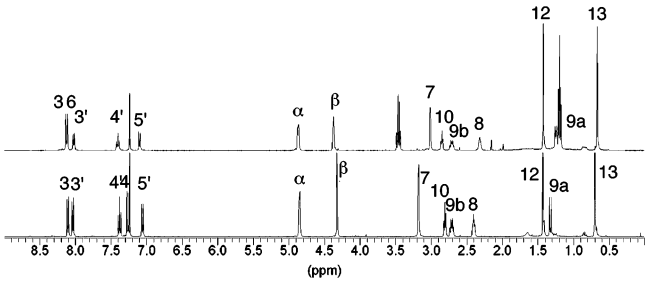

Figure 1. ^{1}H NMR spectra (400 MHz) of products **1** (bottom) and **3** (top). See Chart 2 for numbering.

view of the relative orientation of the pinene and the ferrocenyl groups. The α- and the *β*- protons of the cp ring show almost the same chemical shifts in the two spectra where a broad signal for each α- and *β*-proton is observed.

The presence of ferrocene units in **1**−**3** gives a new absorption band in the visible (Figure 2) due to $\pi-\pi^*$

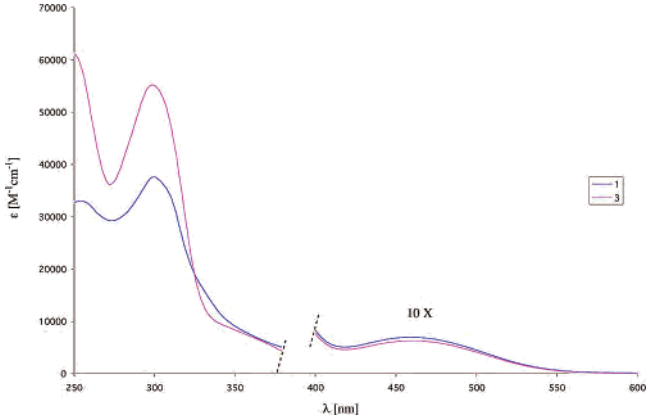

Figure 2. UV−vis spectra of **1** and **3**.

transitions as compared to ferrocene-free CHIRAGEN type ligands.[17] However, as already observed for pinene−bipyridine derivatives, bromo−pinene−bipyridine, or bromo−pinene−terpyridine, bis(pinene−bipyridyl)−6′-[ferrocene] derivatives do not display any CD activity in the visible or near-UV part of the spectrum.

The metal complexes of **1**−**3** are made similarly, starting from $Cu(CH_3CN)_4PF_6$, $AgPF_6$, and $Zn(NO_3)_2$, respectively, as metal sources (Scheme 2). The complexes are made by

Scheme 2

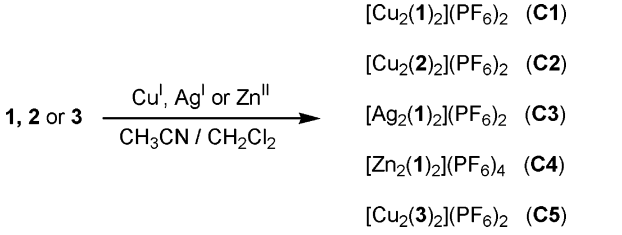

addition of equimolar amounts of the metal and the ligand in a 1:5 mixture acetonitrile−dichloromethane.

The color changes from orange to red (copper case), and it stays orange for the other metal salts. $[Cu_2(\mathbf{1})_2](PF_6)_2$ (**C1**),

(16) Bark, T.; Duggeli, M.; Stoeckli-Evans, H.; Von Zelewsky, A. *Angew. Chem., Int. Ed.* **2001**, *40*, 2848.
(17) Dueggeli, M.; Goujon-Ginglinger, C.; Richard Ducotterd, S.; Mauron, D.; Bonte, C.; Von Zelewsky, A.; Stoeckli-Evans, H.; Neels, A. *Org. Biomol. Chem.* **2003**, 1894.
(18) Luetzen, A.; Hapke, M.; Griep-Raming, J.; Haase, D.; Saak, W. *Angew. Chem., Int. Ed.* **2002**, *41*, 2086.
(19) Perret-Aebi, L.-E.; Von Zelewsky, A. *Synlett* **2002**, *5*, 773.

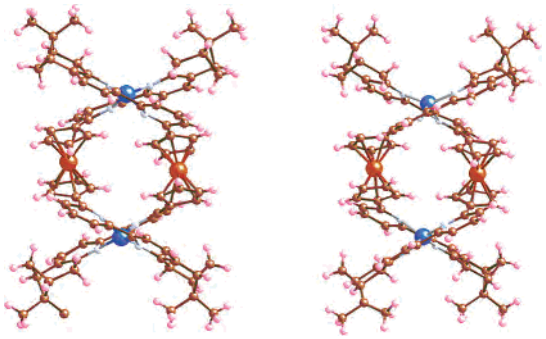

Figure 3. X-ray structures of **C1** (left) and **C2** (right), respectively.

Table 2. Summary of Structural Parameters (Distances and Torsion Angles) and of Configuration of Complexes **C1**−**C3**[a]

entry	compd	ligand	metal	confign	helicity	M···M (Å)	Fe···Fe (Å)	α(bpy$_1$∧bpy$_2$) (deg)
1	**C1**(a)	**1**	Cu	D	*M*	8.08	6.23	63
2	**C1**(b)	**1**	Cu	L	*P*	7.85	6.32	60
3	**C1**(c)	**1**	Cu	L	*P*	7.30	6.30	88
4	**C2**	**2**	Cu	L	*P*	7.94	6.30	63
5	**C3**	**1**	Ag	D	*M*	8.34	6.09	67
6	**C5**	**3**	Cu	L	*P*	7.86	6.32	60

[a] Entries 1−3 are for two different batches of crystallization of **C1** (see text).

$[Cu_2(\mathbf{2})_2](PF_6)_2$ (**C2**), $[Ag_2(\mathbf{1})_2](PF_6)_2$ (**C3**), $[Zn_2(\mathbf{1})_2](PF_6)_4$ (**C4**), and $[Cu_2(\mathbf{3})_2](PF_6)_2$ (**C5**) are directly isolated as hexafluorophosphate salts. The formation of the complexes **C1**−**C5** is quantitative. These complexes were characterized by NMR, ESI-MS, UV−vis, CD, and X-ray structure determinations for **C1**, **C2**, **C3**, and **C5**. Since the absolute configuration of the pinene moiety is known from the product used for synthesis of the ligands, the configuration of the stereogenic elements created in the self-assembly process can be unambiguously determined from the X-ray analysis. The general aspects of molecular structures in all crystals are similar. They show double-stranded helical structures, where the two metal centers lie on the axis of the helix, whereas the ferrocene units connect their "upper" and "lower" part of the structure. The approximate symmetry of all these supramolecular assemblies is C_2.

The complex **C1** was crystallized twice (**C1**(**a**); **C1**(**b**), **C1**(**c**)). The first crystals (**C1**(**a**)) were obtained by slow diffusion of methanol into a solution of the complex in chloroform. From X-ray analysis the structure of the complex was found to be a *M*-double-helix with Δ configuration at the copper centers (Figure 3; more detailed information is reported in Table 2).

The two ferrocene moieties have an eclipsed conformation, and a Δ configuration can be attributed to the iron center. Another batch of crystals, which contain **C1**(**b**) and **C1**(**c**) (Figure 4), was obtained by slow diffusion of toluene into a dichloromethane solution of the complex.

(20) Quinodoz, B.; Stoeckli Evans, H.; Von Zelewsky, A. *Mendeleev Commun.* **2003**, 146.
(21) Enders, M.; Kohl, G.; Pritszkow, H. *J. Organomet. Chem.* **2001**, *622*, 66.
(22) Guo, D.; Han, G.; Duan, C.-Y.; Pang, K.-L.; Meng, Q.-J. *Chem. Commun.* **2002**, 1096.
(23) Bishop, J. J.; Davison, A.; Katcher, M. L.; Lichtenberg, D. W.; Merrill, R. E.; Smart, J. C. *J. Organomet. Chem.* **1971**, *27*, 241.

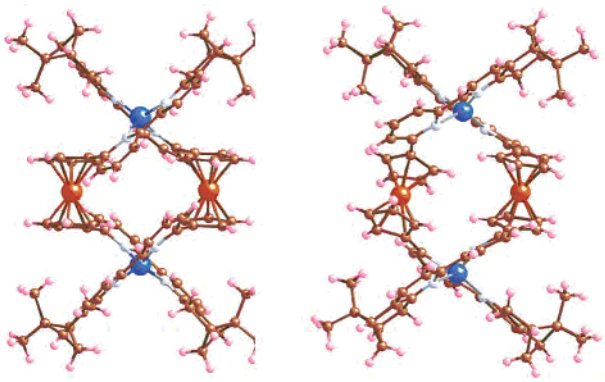

Figure 4. X-ray structures of **C1**(**b**) (left) and **C1**(**C**) (right), respectively.

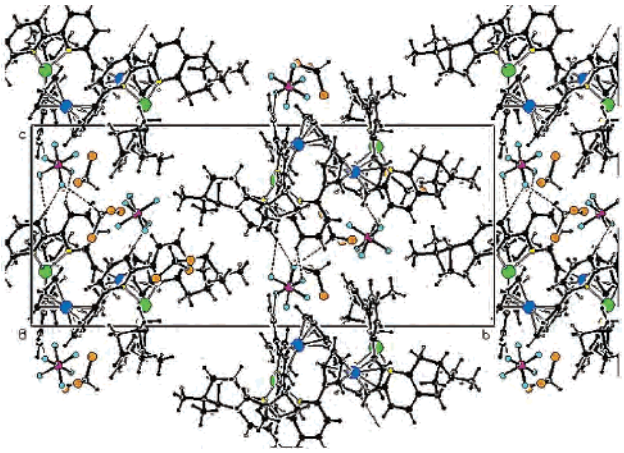

Figure 5. Crystal packing of **C1**(**a**).

The NMR and the CD spectra of the solution were identical with the previous ones, but the X-ray analysis show a different structure in the solid state. Two molecules, both *P*-double-helices with Λ configuration at the copper centers are observed. One of them (**C1**(**c**)) has a dihedral angle in the staggered ferrocene units of 98°, and the other one (**C1**(**b**)) shows 138° for the same angle which implies an eclipsed configuration. Moreover the skew angle between the copper−copper and the ferrocene axes is 26° for **C1**(**b**) and 3° for the complex **C1**(**c**). Also the dihedral angles between the two bipyridines are quite different, namely 60 and 88°, respectively, for **C1**(**b**) and **C1**(**c**). One of the helices has crystallographic C_2 symmetry (**C1**(**b**)) while the other (**C1**(**c**)) shows approximate C_2 symmetry (Figure 4). The configuration of the iron centers in the ferrocene moiety in the complex **C1**(**a**) is Δ and Λ for the complex **C1**(**b**,**c**). The fact that the helices crystallize in two conformers in the same crystal is probably due to the low rotational barrier within the ferrocene unit.

The packing diagram of the complex **C1**(**a**) presented in Figure 5 shows a stabilization of the double-stranded helicate by close C−H···F contacts.

These weak interactions are found mostly between the hexafluorophosphate anions and molecules of chloroform, but the complexes are also linked to the PF_6 through several C−H···F bonds. A chloroform−hexafluorophosphate−complex system is obtained which stabilizes the packing of **C1**(**a**). Bond distances and angles for these close C−H···F

Table 3. Distances, Angles, and Translation Symmetry to Equivalent Position of the C−H···F Interactions of the Complex **C1**(a)

C−H···F bond	C···H (Å)	H···F (Å)	C···F (Å)	α(C−H∧F) (deg)	translation sym
C22−H22···F6	0.9500	2.2900	3.207(15)	164	$2-x, {}^{1}/_{2}+y, 1-z$
C56−H56···F11	0.9500	2.5000	3.348(19)	148	$2-x, -{}^{1}/_{2}+y, 1-z$
C61−H61···F7	0.9500	2.5000	3.429(18)	166	$2-x, -{}^{1}/_{2}+y, 1-z$
C61−H61···F10	0.9500	2.5500	3.272(15)	133	$2-x, -{}^{1}/_{2}+y, 1-z$
C73−H73···F8	0.9500	2.4900	3.432(18)	169	$1-x, -{}^{1}/_{2}+y, -z$
C201−H201···F7	1.0000	2.3700	3.33(2)	161	$2-x, -{}^{1}/_{2}+y, 1-z$
C202−H202···F6	1.0000	2.2500	3.206(17)	161	$1-x, {}^{1}/_{2}+y, 1-z$
C203−H203···F4	1.0000	2.2900	3.19(2)	148	$x, 1+y, z$

contacts are presented in Table 3. The values correspond to those found in the literature. Solvent molecules fill the cavities formed in the crystal.

The analogous silver complex **C3** ($[Ag_2(\mathbf{1})_2]^{2+}$) (Figure 6) can also be obtained in crystalline form (slow diffusion

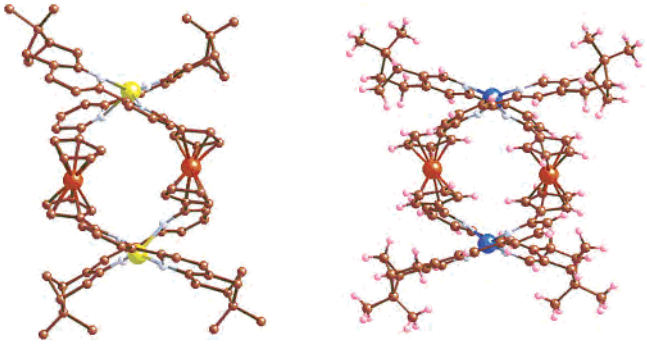

Figure 6. X-ray structure of **C3** (left) and **C5** (right).

of toluene into a dichloromethane solution of the complex). A *M*-double-helix with Δ configuration at the silver centers is observed. Neither another diastereoisomer nor a crystal containing two conformers could be isolated in crystalline form.

Complex **C2** ($[Cu_2(\mathbf{2})_2]^{2+}$) (Figure 3) crystallizes as a *P*-helix (Λ configuration at the copper centers) with a general structure similar to those found for **C1(b)** (Figure 4) and **C3** (Figure 6). The crystals were obtained by slow diffusion of toluene into a dichloromethane solution of the complex.

The X-ray structure of **C5** ($[Cu_2(\mathbf{3})_2]^{2+}$) (Figure 6) indicates that the complex crystallizes as a *P*-helix (Λ configuration at the copper centers) similar to **C1(b)** but with the pinene groups pointing along the helical axis since the complex is derived from the [4,5]pinene−bipyridine. This complex was also obtained by slow diffusion of toluene into a dichloromethane solution of the complex. The general orientation of the molecule is similar to that of the other complexes. No other crystalline forms were isolated.

Besides the study of the crystalline material, CD spectra of complexes **C1**−**C5** were measured to investigate the configuration of the helix also in solution.

The CD spectra observed for **C1** and **C2** (Figure 7) show a positive exciton couplet for **C1** and a negative one for **C2** which can be related to respectively a Λ and a Δ configuration at the metal center. The two CD spectra of both enantiomers **C1** and **C2** are, as expected, mirror images.

Despite complex **C1**(**a**) was obtained in crystalline form as a *P*-helix with a Δ configuration at the metal center, its CD spectrum shows a positive exciton couplet indicating the presence of the other diastereoisomer in solution, thus possessing a Λ configuration at the metal center. NMR studies confirm that it was the minor species which was crystallized. The CD spectrum of **C1**(**b**,**c**) presents also a positive exciton coupling (Λ configuration at the metal center) which is in agreement with the X-ray structure obtained.

The zinc complex $[Zn_2(\mathbf{1})_2](PF_6)_2$ (**C4**) presents also a positive couplet (Figure 8) as in the copper case (**C1**). This can be related to a Λ configuration. Surprisingly, the silver complex $[Ag_2(\mathbf{1})_2](PF_6)_2$ (**C3**) based, as in the case of **C1** and **C4**, on a (*R*,*R*)-(−)-pinene−bipyridine derivative, shows a negative exciton couplet representing a Δ configuration at the metal center (Figure 8). This inversion of the configuration is difficult to explain. The size difference of the metal cations (Ag^+ $r = 126$ pm; Zn^{2+} $r = 76$ pm) could play a role; it could force ferrocene to adopt a distorted configuration, leading to the other diastereoisomer. The CD spectrum of the complex **C5**, $[Cu_2(\mathbf{2})_2](PF_6)_2$, shows a positive exciton couplet (Figure 8) which corresponds to a Λ configuration at the metal center which is again in agreement with the other configurations of **C1** and **C4**.

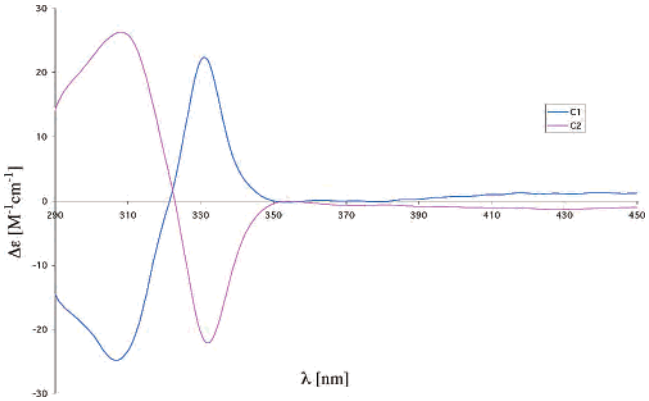

Figure 7. CD spectra of **C1** and **C2**.

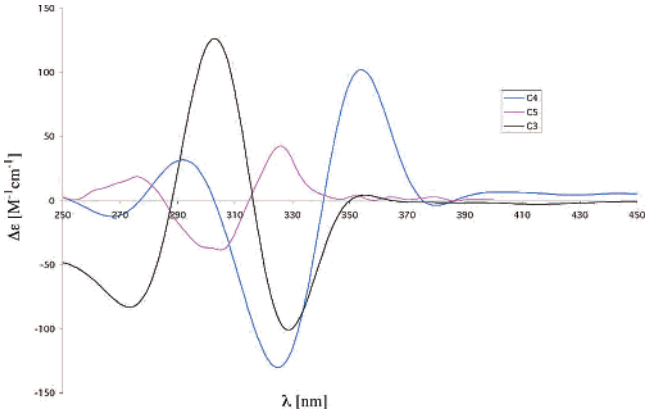

Figure 8. CD spectra of **C3**−**C5**.

Scheme 3 Synthesis of the Alkylated Ligands **1a**−**c**

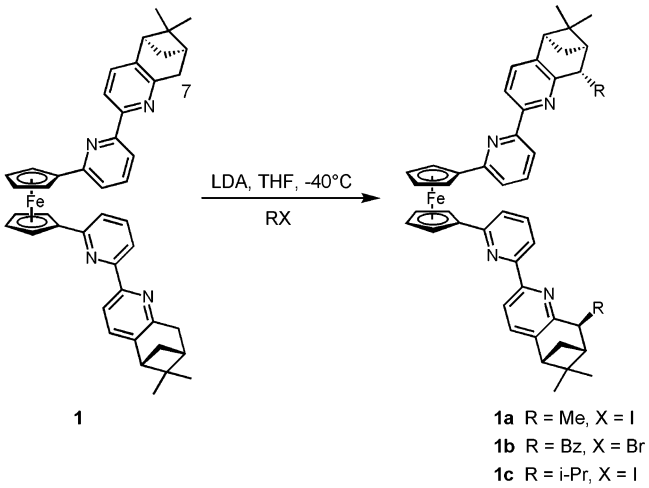

Table 4. Results of the Synthesis for **1a**−**c**

entry	starting ligand	alkylating reagent	ligand	yield (%)
1	**1**	MeI	**1a**	95
2	**1**	BzBr	**1b**	60
3	**1**	i-PrI	**1c**	85

The conclusion of these CD experiments is that the complexes are not formed in a completely stereoselective way since the two diastereomers are formed. Moreover the configuration of the complex in solution does not necessarily correspond to the configuration in the solid state; i.e., the minor form can be crystallized as well as the major one.

To study the diastereoselective induction of ligand **1**, three different alkylated compounds were synthesized (Scheme 3). Due to the acidity of the proton on position 7 of the pinene group, the anion is formed selectively and stereospecifically. Subsequently, an alkylating agent is added to the mixture leading to the bis(7-alkylated-(*R*,*R*)-(−)-[5,6]pinene−bipyridyl)−6′-[ferrocene], **1a**−**c**.

The results obtained for the synthesis of the ligands is presented in Table 4.

The NMR spectra of **1a**−**c** present the same general feature. The α-protons of the Cp ring are split since interactions with the pinene make them nonequivalent. The other protons are only shifted to slighly higher or lower field as shown in Figure 9, but no drastic variations occur.

The UV−vis spectra of the ligands **1a**−**c** are very similar to that of **1**. The intensities obtained are about the same, and the main band in the visible is always at 460 nm (Figure 10). As in the case of **1**, the ligands **1a**−**c** are void of CD activity in the visible or near-UV part of the spectrum.

ESI-MS analyses always show the molecular peak of the ligand with a 100% intensity. No other significant signals are observed in the spectrum.

Ligands **1a**−**c** were complexed with copper(I) using a method identical with that applied for **1**, leading to the alkylated complexes **C6**−**C8** (Scheme 4).

ESI-MS analyses confirmed immediately that similar assemblies as in the case of **C1** and **C2** were present. Double-stranded helicates are obtained for the complexes $[Cu_2(\mathbf{1a})_2](PF_6)_2$ (**C6**), $[Cu_2(\mathbf{1b})_2](PF_6)_2$ (**C7**), $[Cu_2(\mathbf{1a})_2](PF_6)_2$ (**C6**), and $[Cu_2(\mathbf{1c})_2](PF_6)_2$ (**C8**). The signal corresponding to

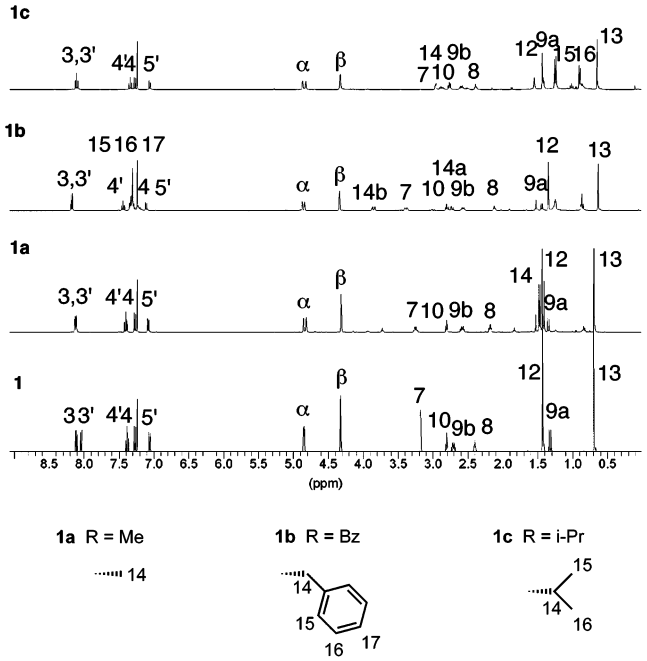

Figure 9. ^{1}H NMR spectra of **1** and **1a**−**c**. See Chart 2 for numbering of **1**.

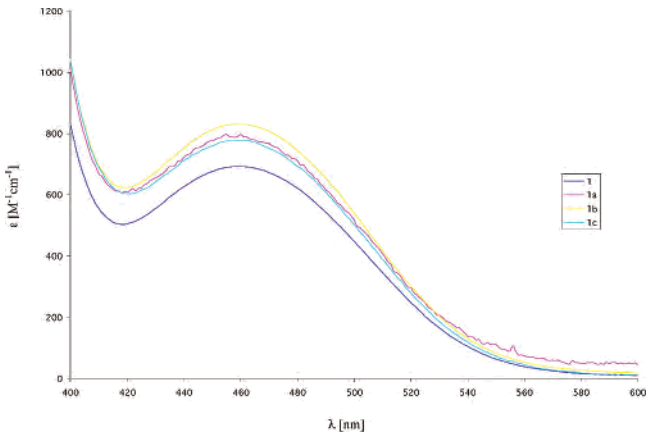

Figure 10. UV−vis spectra of **1** and **1a**−**c**.

$[Cu_2L_2]^{2+}$ is very intense, and it presents the correct isotopic pattern for a 2+ charged compound in each case.

The comparison of the NMR spectra of **C6**−**C8** and **C1** presented in Figure 11 show the presence of the two diastereomers.

The results of the integration process are summarized in Table 5.

Although the NMR investigation shows a moderate diastereoselectivity for all these alkylated ligands, quite different values for the CD spectra are observed (Figure 12). This must be due to different distortions of the bipyridine units in the coordination sphere.

In conclusion, the synthesis of several new enantiopure redox active ligands containing ferrocenyl groups (**1**−**3**) has been accomplished. These ligands were thoroughly characterized by standard methods (NMR, MS, X-ray). These ligands show interesting self-assembly properties leading to double-stranded helicates (**C1**−**C8**) with various metal ions such as Cu(I), Ag(I), and Zn(II). Some of these molecular

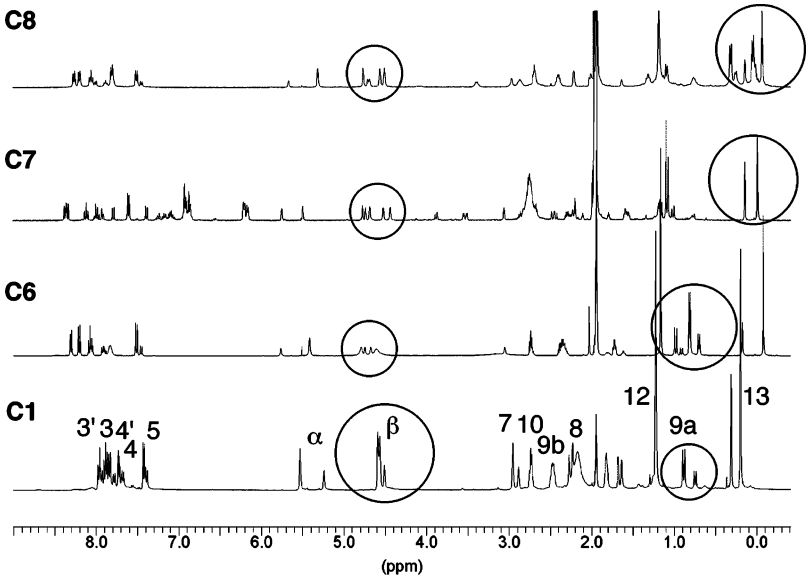

Figure 11. ^{1}H NMR of the complexes **C1** and **C6**−**C8**.

Scheme 4. Synthesis of the Copper Complexes **C6**−**C8**

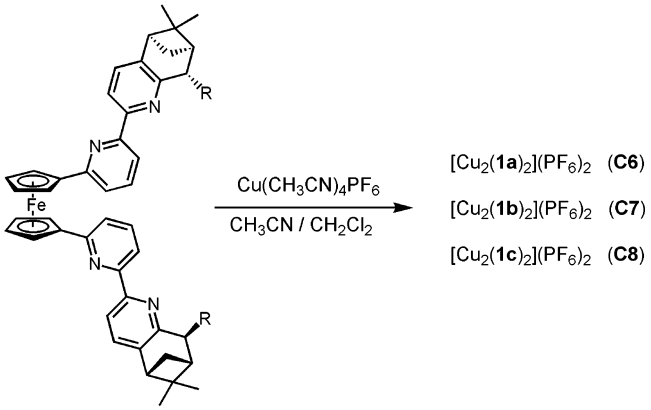

1a R = Me
1b R = Bz
1c R = i-Pr

Table 5. Results Obtained for **C6**−**C8**

entry	complex	alkyl group	de (%)
1	**C1**	−	68
2	**C6**	Me	73
3	**C7**	Bz	59
4	**C8**	i-Pr	71

architectures could be studied by X-ray crystallography in the solid state. Spectroscopic investigations in solution demonstrated in most cases a lack of complete diastereoselectivity of the self-assembling process; i.e., mixtures of *M*- and *P*-helices, respectively, are formed.

Experimental Section

Chemicals and Starting Materials. All chemicals, solvents, and reagent grade products were obtained from Fluka, Aldrich, Merck, Acros, or Strem chemicals and used, unless otherwise stated, without further purification. Pyridine was dried over KOH and freshly distilled prior to use. Dry ammonium acetate was dried for several days in a vacuum oven at 40 °C. Diethyl ether and THF were distilled from sodium/benzophenone prior to use. Hexane was dried over CaH_2 and distilled prior to use. When ferrocene was involved in the reaction, solvents were degassed prior to use.

Measurements. NMR spectra were recorded on a Varian Gemini 300 (300.075 MHz) or on a Bruker Avance DRX400 (400.13 MHz) spectrometer, chemical shifts are given in ppm using the solvent itself as internal standard, and coupling constants *J* are given in hertz. Attribution of the ^{1}H and ^{13}C signals was performed by ^{1}H,^{1}H-COSY, DEPT, and ^{1}H−^{13}C-HECTOR techniques. The diastereotopic protons at carbon 9 are labeled as H_a for the *endo*-oriented protons and H_b for the *exo*-oriented protons. The *exo* methyl groups of the pinene moieties are assigned as 12, and the *endo* oriented ones as 13. The numbering arrangements for the ligands are shown in the charts. Mass spectral data were acquired (a) on a VG Instrument 7070E equipped with a FAB inlet system, (b) on a Hewlett-Packard 5988A quadrupol mass spectrometer with an electron ionization (EI) source, and (c) on a Bruker FTMS 4.7 T BioApex II using a standard electrospray ion source (ESI). UV/visible spectra were measured on a Perkin-Elmer Lambda 40 spectrometer. Wavelengths are given in nm, and molar absorption coefficients (ϵ), in M^{-1} cm^{-1}. Circular dichroism (CD) spectra were recorded on a Jasco J-715 spectropolarimeter, and the results are given in $\Delta\epsilon$ (M^{-1} cm^{-1}). X-ray measurements were carried out at the University of Neuchâtel, Neuchâtel, Switzerland. X-ray data are presented in Tables 6 and 7.

Synthesis of Bis((*R*,*R*)-(−)-[5,6]pinene−bipyridyl)−[1,1′-ferrocene] (1). A suspension of the dilithioferrocene−TMEDA adduct

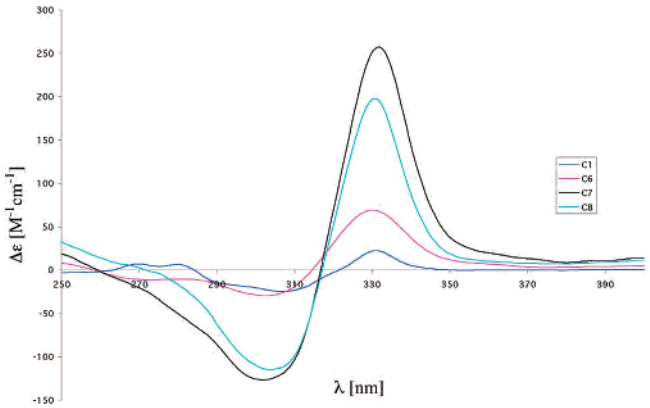

Figure 12. CD spectra of **C1** and **C6**−**C8**.

Table 6. X-ray Data for **C1**(a−c) and **C2**

	C1(a)	**C1**(b,c)	**C2**
empirical formula	$[Cu_2Fe_2(C_{22}H_{21}N_2)_4]$-$(PF_6)_2(CHCl_3)_3(CH_3OH)_{4.5}$	$[Cu_2Fe_2(C_{22}H_{21}N_2)_4]$-$(PF_6)_4(CH_2Cl_2)_{5.25}$	$[Cu_2Fe_2(C_{22}H_{21}N_2)_4]$-$(PF_6)_4(CH_2Cl_2)_{8.5}$
fw	2284.74	2518.24	2794.28
cryst color, habit	orange, plate	red, block	red, block
cryst size (mm)	0.50 × 0.50 × 0.15	0.50 × 0.40 × 0.40	0.40 × 0.20 × 0.10
cryst system	monoclinic	monoclinic	orthorhombic
space group	$P2_1$	C_2	$P2_12_12_1$
a (Å)	13.3902(7)	22.7441(13)	16.1399(6)
b (Å)	31.172(2)	24.1082(14)	19.5241(7)
c (Å)	14.3665(9)	29.033(2)	33.5507(10)
α (deg)	90	90	90
β (deg)	109.671(7)	106.965(7)	90
γ (deg)	90	90	90
V (Å^3)	5646.6(6)	15 226.6(16)	10 572.4(6)
Z	2	4	4
D_{calc} (g/cm^3)	1.341	1.091	1.543
abs coeff (mm^{-1})	0.933	0.692	1.195
F(000)	2334	5092	4996
θ min and max (deg)	2.08−25.99	1.65−26.05	1.21−24.96
reflections collected/unique	44 533/21 768	60 599/29 344	66 853/18 351
refinement method	full-matrix least squares on F^2	full-matrix least squares on F^2	full-matrix least squares on F^2
final R indices [$I > 2\sigma(I)$]	R1 = 0.0753 wR2 = 0.1428	R1 = 0.0603 wR2 = 0.1275	R1 = 0.0846 wR2 = 0.2192
R indices all data	R1 = 0.2023 wR2 = 0.1833	R1 = 0.1316 wR2 = 0.1453	R1 = 0.1053 wR2 = 0.2324

Table 7. X-ray Data for **C3** and **C5**

	C3	**C5**
empirical formula	$[Ag_2Fe_2(C_{22}H_{21}N_2)_4](ClO_4)_2(CH_2Cl_2)_3$	$[Cu_2Fe_2(C_{22}H_{21}N_2)_4](PF_6)_2(CH_2Cl_2)_2(C_7H_8)_3$
fw	2034.83	2228.71
cryst color, habit	yellow, plate	red, block
cryst size (mm)	0.20 × 0.20 × 0.05	0.30 × 0.25 × 0.20
cryst system	monoclinic	monoclinic
space group	$P2_1$	$P2_1$
a (Å)	17.718(5)	11.8843(8)
b (Å)	13.533(2)	27.3956(14)
c (Å)	21.447(4)	16.7683(13)
α (deg)	90	90
β (deg)	96.38(2)	110.565(8)
γ (deg)	90	90
V (Å^3)	5110.7(19)	5111.5(6)
Z	2	2
D_{calc} (g/cm^3)	1.322	1.448
abs coeff (mm^{-1})	0.917	0.90
F(000)	2076	2300
θ min and max (deg)	0.82−25.26	1.97−25.94
reflcns collcd/unique	19 472/14 631	40 439/19 532
refinement method	full-matrix least squares on F^2	full-matrix least squares on F^2
final R indice [$I > 2\sigma(I)$]	R1 = 0.1155 wR2 = 0.1935	R1 = 0.0478 wR2 = 0.1095
R indices all data	R1 = 0.2998 wR2 = 0.2545	R1 = 0.0620 wR2 = 0.1138

(5 mmol) in THF (30 mL) was cooled to 0 °C, and a solution of $ZnCl_2$ (1.363 g, 10 mmol) in THF (20 mL) was added. The resulting orange slurry was allowed to stir over 1.5 h at RT (room temperature). In a separate flask $(PPh_3)_2PdCl_2$ (175 mg, 0.25 mmol) was suspended in THF (8 mL), to which was added dropwise DIBAL-H solution (1.1 mL, 0.5 M, 0.55 mmol) in THF. This gave a homogeneous dark solution which was added to the 1,1′-bis-(chlorozinc)ferrocene via syringe. 6′-Bromo-[5,6]pinenebpy (4.115 g, 12.5 mmol) in THF (40 mL) was added dropwise via syringe, and the resulting suspension was stirred for 5 days. During this time its color changed from brown to red-brown. The reaction was checked by TLC, and after 3 days some catalyst was readded if necessary. Then the reaction mixture was quenched by adding 7.5 M NaOH (60 mL). After 2 h of stirring the organic layer was separated from the water fraction, which was extracted twice with dichloromethane (30 mL). The combined organic layers were dried over $MgSO_4$, filtered, and evaporated to dryness. Purification by column chromatography of silica (7:1 hexane/AcOEt) gave the desired product (**1**) (900 mg, 26%) as an orange powder. ^{1}H NMR (400 MHz, $CDCl_3$, δ): 8.11 (d, 2H, H(3), $^3J_{3,4}$ = 7.58 Hz); 8.03 (d, 2H, H(3′), $^3J_{3',4'}$ = 7.7 Hz); 7.38 (dd, 2H, H(4′), $^3J_{4',3'}$ = 7.7 Hz, $^3J_{4',5'}$ = 7.7 Hz); 7.25 (d, 2H, H(4), $^3J_{4,3}$ = 7.7 Hz); 7.05 (d, 2H, H(5′), $^3J_{5',4'}$ = 7.7 Hz); 4.85 (4H, H(α)); 4.32 (4H, H(β)); 3.17 (d, 4H, H(7), $^3J_{7,8}$ = 2.78 Hz); 2.8 (dd, 2H, H(10), $^3J_{10,9b}$ = 5.4 Hz, $^4J_{10,8}$ = 5.75 Hz); 2.71 (ddd, 2H, H(9_b), $^2J_{9b,9a}$ = 9.95 Hz, $^3J_{9b,8}$ = 5.4 Hz, $^3J_{9b,10}$ = 5.4 Hz); 2.4 (ddt, 2H, H(8), $^3J_{8,9a}$ = 5.4 Hz, $^4J_{8,10}$ = 5.75 Hz, $^3J_{8,7}$ = 2.78 Hz); 1.42 (s, 6H, H(12)); 1.32 (d, 2H, H(9a), $^2J_{9a,9b}$ = 9.95); 0.69 (s, 6H, H(13)). ^{13}C NMR (100 MHz, $CDCl_3$, δ): 156.78 (Cq, C(2)); 155.7 (Cq, C(2′)); 155.4 (Cq, C(6)); 153.6 (Cq, C(6′)); 141.59 (Cq, C(5)); 136.2 (CH, C(4′)); 133.3 (CH, C(4)); 119.1 (CH, C(5′)); 117.7 (CH, C(3)); 117.0 (CH, C(3′)); 85.21 (Cq, C(1″, 1‴); 70.5 (CH, C(β)); 68.5 (CH, C(α)); 46.3 (CH,

C(10)); 40.0 (CH, C(8)); 39.2 (Cq, C(11)); 36.4 (CH_2, C(7)); 31.7 (CH_2, C(9)); 25.8 (CH_3, C(12)), 21.1 (CH_3, C(13)). HRMS-ESI: m/z = 683.28 ($(M + H)^+$, 100%). UV−vis ($CHCl_3$) [λ (ϵ)]: 460 nm (700); 300 nm (3.8×10^4).

Synthesis of Bis((*S*,*S*)-(+)-[5,6]pinene−bipyridyl)−[1,1′-ferrocene] (2). A suspension of the dilithioferrocene−TMEDA adduct (4.8 mmol) in THF (30 mL) was cooled to 0 °C, and a solution of $ZnCl_2$ (1.3 g, 10 mmol) in THF (20 mL) was added. The resulting orange slurry was stirred during 1.5 h at RT. In a separate flask $(PPh_3)_2PdCl_2$ (168 mg, 0.24 mmol) was suspended in THF (8 mL), to which was added dropwise DIBAL-H solution (1.1 mL, 0.5 M, 0.55 mmol) in THF. This gave a homogeneous dark solution, which was added to the 1,1′-bis(chlorozinc)ferrocene via syringe. 6′-Bromo-(*S*,*S*)-(+)-[5,6]-pinenebpy (3.95 g, 12 mmol) in THF (40 mL) was added dropwise via syringe, and the resulting suspension was stirred for 5 days, during which its color changed from brown to red-brown. The reaction is checked by TLC, and after 3 days some catalyst was readd if necessary. Then the reaction mixture was quenched by adding 7.5 M NaOH (60 mL). After 2 h of stirring the organic layer was separated from the water fraction, which was extracted twice with dichloromethane (30 mL). The combined organic layers were dried over $MgSO_4$, filtered, and evaporated to dryness. Purification by column chromatography of silica (7:1 hexane/AcOEt) gave the desired product (**2**) (600 mg, 18%) as an orange powder. For analytical data, see **1**.

Synthesis of Bis((*R*,*R*)-(−)-[4,5]pinene−bipyridyl)−[1,1′-ferrocene] (3). A suspension of the dilithioferrocene−TMEDA adduct (5 mmol) in THF (30 mL) was cooled to 0 °C, and a solution of $ZnCl_2$ (1.363 g, 10 mmol) in THF (20 mL) was added. The resulting orange slurry stirred during 1.5 h at RT. In a separate flask $(PPh_3)_2$-$PdCl_2$ (175 mg, 0.25 mmol) was suspended in THF (8 mL), to which was added dropwise DIBAL-H solution (1.1 mL, 0.5 M, 0.55 mmol) in THF. This gave a homogeneous dark solution which was added to the 1,1′-bis(chlorozinc)ferrocene via syringe. 6′-Bromo-[4,5]pinenebpy (3.62 g, 11 mmol) in THF (40 mL) was added dropwise via syringe, and the resulting suspension was stirred for 5 days, during which its color changed from brown to red-brown. The reaction was checked by TLC, and after 3 days some catalyst was readd if necessary. Then the reaction mixture was quenched by adding 7.5 M NaOH (60 mL). After 2 h of stirring the organic layer was separated from the water fraction, which was extracted twice with dichloromethane (30 mL). The combined organic layers were dried over $MgSO_4$, filtered, and evaporated to dryness. Purification by column chromatography of silica (7:1 hexane/AcOEt) gave the desired product (**3**) (692 mg, 20%) as an orange powder. ^{1}H NMR (400 MHz, $CDCl_3$, δ): 8.19 (s, 2H, H (3)); 8.15 (s, 2H, H (6)); 8.07 (d, 2H, H (3′), $^3J_{3',4'}$ = 7.6 Hz); 7.45 (dd, 2H, H (4′), $^3J_{4',3'}$ = 7.6 Hz, $^3J_{4',5'}$ = 7.6 Hz); 7.14 (d, 2H, H (5′), $^3J_{5',4'}$ = 7.6 Hz); 4.92 (4H, H (α)); 4.41 (4H, H (β)); 3.05 (d, 4H, H (7), $^3J_{7,8}$ = 1.8 Hz); 2.89 (dd, 2H, H (10), $^3J_{10,9b}$ = 5.4 Hz, $^4J_{10,8}$ = 5.4 Hz); 2.75 (ddd, 2H, H (9_b), $^2J_{9b,9a}$ = 9.4 Hz, $^3J_{9b,10}$ = 5.4 Hz, $^3J_{9b,8}$ = 5.4 Hz); 2.32 (ddt, 2H, H (8), $^3J_{8,9a}$ = 5.4 Hz, $^4J_{8,10}$ = 5.4 Hz, $^3J_{8,7}$ = 1.8 Hz); 1.41 (s, 6H, H (12)); 1.25 (d, 2H, H (9_a), $^2J_{9a,9b}$ = 9.4 Hz); 0.65 (s, 6H, H (13)). ^{13}C NMR (100 MHz, $CDCl_3$, δ): 157.2 (Cq); 156.0 (Cq); 155.1 (Cq); 145.7 (CH, C(6)); 145.5 (Cq); 143.1 (Cq); 137.0 (CH, C(4′)); 120.9 (CH, C(3)); 120.0 (CH, C(5′)); 117.8 (CH, C(3′)); 85.8 (Cq); 71.1 (CH, C(β)); 69.4 (CH, C(α)); 45.0 (CH, C(10)); 40.6 (CH, C(8)); 39.7 (Cq, C(11)); 33.4 (CH_2, C(7)); 32.3 (CH_2, C(9)); 26.5 (CH_3, C(12)); 21.9 (CH_3, C(13)). ESI-MS: m/z = 683.32 ($(M + H)^+$, 100%). UV−vis (CH_3-CN) [λ (ϵ)]: 460 nm (627); 299 nm (5.5×10^4); 249 nm (6.1×10^4).

Synthesis of Bis(7-dimethyl-(*R*,*R*)-(−)-[5,6]pinene−bipyridyl)−[1,1′-ferrocene] (1a). A Schlenk flask under argon was charged with dry THF (2 mL) and diisopropylamine (0.42 mL, 3 mmol). The reaction mixture was cooled to −40 °C, and n-BuLi (1 mL, 1.55 M in hexane, 1.55 mmol) was rapidely added via syringe. The solution was allowed to warm to 0 °C and was kept for 30 min at this temperature. Then the system was cooled again to −40 °C and bis((*R*,*R*)-(−)-[5,6]pinene−bipyridyl)−[1,1′-ferrocene] (**1**) (150 mg, 0.22 mmol) dissolved in dry THF (4 mL) was added dropwise within 1 h via a syringe pump. Directly after addition of the first drop of this solution, the reaction media turned to green and then to dark blue. After addition of **1**, the dark blue solution was kept at −40 °C for 2 h. Subsequently methyl iodide (0.125 mL, 2 mmol) was added via a syringe pump within 1 h. After this addition the reaction mixture was allowed to warm to room temperature overnight. During this time the dark blue color turned to brown-orange. The mixture was quenched with water (2 mL) and the THF evaporated. More water was added, and the mixture was extracted with CH_2Cl_2. The organic phase was dried over $MgSO_4$ and filtered off. After removal of the solvent, the residue was purified by column chromatography (SiO_2; 7:1:0.1 hexane/ethyl acetate/TEA). Pure **1a** (140 mg, 95%) as an orange solid was obtained. ^{1}H NMR (400 MHz, $CDCl_3$, δ): 8.12 (dd, 4H, H(3, 3′), $^3J_{3,4}$ = 7.58 Hz, $^3J_{3',4'}$ = 7.83 Hz); 7.40 (dd, 2H, H(4′), $^3J_{4',3'}$ = 7.83 Hz, $^3J_{4',5'}$ = 7.83 Hz); 7.26 (d, 2H, H(4), $^3J_{4,3}$ = 7.58 Hz); 7.07 (d, 2H, H(5′), $^3J_{5',4'}$ = 7.83 Hz); 4.82 (4H, H(α)); 4.31 (4H, H(β)); 3.26 (m, 2H, H(7); 2.80 (dd, 2H, H(10), $^3J_{10,9b}$ = 5.4 Hz, $^4J_{10,8}$ = 5.75 Hz); 2.58 (ddd, 2H, H(9_b), $^2J_{9b,9a}$ = 9.95 Hz, $^3J_{9b,8}$ = 5.75 Hz, $^3J_{9b,5}$ = 5.4 Hz); 2.19 (ddt, 2H, H(8), $^3J_{8,9a}$ = 5.75 Hz, $^4J_{8,10}$ = 5.75 Hz, $^3J_{8,7}$ = 2.78 Hz); 1.47 (d, 6H, H(14), $^3J_{14,7}$ = 7.07 Hz); 1.43 (s, 6H, H(12)); 1.34 (d, 2H, H(9a), $^2J_{9a,9b}$ = 9.95 Hz); 0.69 (s, 6H, H(13)). ^{13}C NMR (100 MHz, $CDCl_3$, δ): 159.9 (Cq, C(2)); 156.8 (Cq, C(2′)); 155.9 (Cq, C(6)); 153.7 (Cq, C(6′)); 141.7 (Cq, C(5)); 136.5 (CH, C(4′)); 133.3 (CH, C(4)); 119.4 (CH, C(5′)); 117.9 (CH, C(3)); 117.4 (CH, C(3′)); 85.6 (Cq, C(1″)); 70.9 (CH, C(β)), 69.0 (CH, C(α)); 47.2 (CH, C(10)); 46.9 (CH, C(8)); 41.5 (Cq, C(11)); 38.9 (CH, C(7)); 28.7 (CH_2, C(9)); 26.4 (CH_3, C(13)); 21.0 (CH_3, C(12)), 18.3 (CH_3, C(14)). ESI-MS: m/z = 711.33 ($(M + H)^+$, 100%). UV−vis ($CHCl_3$) [λ (ϵ)]: 457 nm (796); 300 nm (3.9×10^4); 256 nm (2.9×10^4).

Synthesis of Bis(7-dibenzyl-(*R*,*R*)-(−)-[5,6]pinene−bipyridyl)−[1,1′-ferrocene] (1b). A Schlenk flask under argon was charged with dry THF (2 mL) and diisopropylamine (0.15 mL, 1.1 mmol). The reaction mixture was cooled to −40 °C, and n-BuLi (0.34 mL, 1.55 M in hexane, 0.52 mmol) was rapidly added via syringe. The solution was allowed to warm to 0 °C and was kept for 30 min at this temperature. Then the system was cooled again to −40 °C and bis((*R*,*R*)-(−)-[5,6]pinene−bpy)−[1, 1′-ferrocene] (**1**) (100 mg, 0.147 mmol) dissolved in dry THF (4 mL) was added dropwise within 1 h via a syringe pump. Directly after addition of the first drop of this solution, the reaction media turned to green and then to dark blue. After addition of **1**, the dark blue solution was kept at −40 °C for 2 h. Subsequently benzyl bromide (0.14 mL, 1.2 mmol) was added via a syringe pump within 1 h. After this addition the reaction mixture was allowed to warm to room temperature overnight. During this time the dark blue color turned to brown-orange. The mixture was quenched with water (2 mL) and the THF evaporated. More water was added, and the mixture was extracted with CH_2Cl_2. The organic phase was dried over $MgSO_4$ and filtered off. After removal of the solvent, the residue was purified by column chromatography (SiO_2; 7:1:0.1 hexane/ethyl acetate/TEA). Pure **1b** (76 mg, 60%) as an orange solid was obtained. ^{1}H NMR (400 MHz, $CDCl_3$, δ): 8.19 (d, 4H, H(3), H(3′), $^3J_{3,4}$ = 7.83 Hz, $^3J_{3',4'}$ =7.83

Hz); 7.42 (dd, 2H, H(4′), $^3J_{4',3'}$ = 7.83 Hz, $^3J_{4',5'}$ = 7.83 Hz); 7.35−7.25 (m, 10H, H(15), H(16), H(17)); 7.24 (d, 2H, H(4), $^3J_{4,3}$ = 7.83 Hz); 7.11 (d, 2H, H(5′), $^3J_{5',4'}$ = 7.83 Hz); 4.86 (4H, H(α)); 4.34 (4H, H(*β*)); 3.85 (dd, 2H, H(14b), $^2J_{14b,14a}$ = 13.45 Hz, $^3J_{14b,7}$ = 3.66 Hz), 3.39 (ddd, 2H, H(7), $^3J_{7,8}$ = 5.81 Hz, $^3J_{7,14b}$ = 3.36 Hz, $^3J_{7,14a}$ = 1.11 Hz); 2.8 (dd, 2H, H(10), $^3J_{10,9b}$ = 5.31 Hz, $^4J_{10,8}$ = 5.81 Hz); 2.75 (dd, 2H, H(14a), $^2J_{14a,14b}$ = 13.39 Hz, $^3J_{14a,7}$ = 1.11 Hz); 2.55 (m, 2H, H(9b)), 2.13 (ddd, 2H, H(8), $^3J_{8,9a}$ = 2.27 Hz, $^4J_{8,10}$ = 5.81 Hz, $^3J_{8,7}$ = 5.81 Hz); 1.44 (d, 2H, H(9a), $^2J_{9a,9b}$ = 9.6 Hz); 1.34 (s, 6H, H(12)), 0.63 (s, 6H, H(13)). ^{13}C NMR (100 MHz, $CDCl_3$, *δ*): 158.5 (Cq); 156.9 (Cq); 155.8 (Cq); 153.67 (Cq); 141.3 (Cq); 136.5 (CH, C(4′)); 133.5−128.3 (CH, C(15), C(16), C(17)); 125.8 (CH, C(4)); 119.5 (CH, C(5′)); 118.2 (CH, C(3)); 117.4 (CH, C(3′)); 85.8 (Cq, C(1″)); 70.9 (CH, C(*β*)), 68.9 (CH, C(α)); 47.0 (CH, C(10)); 46.3 (CH, C(7)); 42.6 (CH, C(8)); 41.2 (Cq, C(6)); 38.8 (CH_2, C(14)); 28.5 (CH_2, C(9)); 26.3 (CH_3, C(13)); 20.9 (CH_3, C(12)). ESI-MS: *m*/*z* = 863.37 ((M + H)$^+$, 100%). UV−vis ($CHCl_3$) [*λ* (*ϵ*)]: 459 nm (830); 310 nm (3.5 × 10^4); 251 nm (3.2 × 10^4).

Synthesis of Bis(7-diisopropyl-(*R*,*R*)-(−)-[5,6]pinene−bipyridyl)−[1,1′-ferrocene] (1c). A Schlenk flask under argon was charged with dry THF (2 mL) and diisopropylamine (0.5 mL, 3.5 mmol). The reaction mixture was cooled to −40 °C, and n-BuLi (1.68 mL, 1.55 M in hexane, 2.6 mmol) was rapidely added via syringe. The solution was allowed to warm to 0 °C and was kept for 30 min at this temperature. Then the system was cooled again to −40 °C, and bis((*R*,*R*)-(−)-[5,6]pinene−bpy)−[1,1′-ferrocene] (**1**) (200 mg, 0.293 mmol) dissolved in dry THF (4 mL) was added dropwise within 1 h via a syringe pump. Directly after addition of the first drop of this solution, the reaction media turned to green and then to dark blue. After addition of **1**, the dark blue solution was kept at −40 °C for 2 h. Subsequently isopropyl iodide (0.147 mL, 1.47 mmol) was added via a syringe pump within 1 h. After this addition the reaction mixture was kept at −40 °C during 12 h and then allowed to warm to room temperature overnight. During this time the dark blue color turned to brown-orange. The mixture was quenched with water (2 mL) and the THF evaporated. More water was added, and the mixture was extracted with CH_2Cl_2. The organic phase was dried over $MgSO_4$ and filtered off. After removal of the solvent, the residue was purified by column chromatography (SiO_2; 6:1 hexane/CH_2Cl_2, R_f = 0.8). Pure **1c** (191 mg, 85%) as an orange solid was obtained. ^{1}H NMR (400 MHz, $CDCl_3$, *δ*): 8.10 (d, 4H, H(3, 3′), $^3J_{3,4}$ = 4.6 Hz, $^3J_{3',4'}$ = 7.6 Hz); 7.33 (dd, 2H, H(4′), $^3J_{4',3'}$ = 7.6 Hz, $^3J_{4',5'}$ = 7.6 Hz); 7.27 (d, 2H, H(4), $^3J_{4,3}$ = 4.6 Hz); 7.05 (d, 2H, H(5′), $^3J_{5',4'}$ = 7.6 Hz); 4.84 (4H, H(α)); 4.32 (4H, H(*β*)); 2.96 (m, 2H, H(7); 2.87 (m, 2H, H(14)); 2.78 (m, 2H, H(10)); 2.59 (m, 2H, H(9_b)); 2.39 (m, 2H, H(8)); 1.43 (s, 6H, H(12)); 1.42 (d, 2H, H(9a), $^2J_{9a,9b}$ = 9.5 Hz); 1.24(d, 6H, H(15), $^3J_{15,14}$ = 7.0 Hz); 0.89 (d, 6H, H(16), $^3J_{16,14}$ = 7.0 Hz); 0.63 (s, 6H, H(13)). ^{13}C NMR (100 MHz, $CDCl_3$, *δ*): 158.5 (Cq); 157.1 (Cq); 156.4 (Cq); 153.4 (Cq); 136.4 (CH, C(4′)); 133.3 (CH, C(4)); 119.8 (CH, C(5′)); 118.4 (CH, C(3)); 117.6 (CH, C(3′)); 85.6 (Cq, C(1″)); 72.3 (CH, C(*β*)), 68.8 (CH, C(α)); 49.2 (CH, C(7)); 46.8 (CH, C(10)); 42.0 (CH, C(8)); 41.5 (Cq); 30.5 (CH, C(14)); 29.5 (CH_2, C(9)); 26.4 (CH_3, C(12)); 22.4 (CH_3, C(15)); 21.1 (CH_3, C(13)), 20.3 (CH_3, C(16)). ESI-MS: *m*/*z* = 767.38 ((M + H)$^+$, 100%). UV−vis (CH_2Cl_2) [*λ* (*ϵ*)]: 459 nm (778); 300 nm (3.8 × 10^4); 252 nm (3.7 × 10^4).

Complex Synthesis. Typical Procedure. In a typical procedure the bis(pinene−bipyridyl)−[ferrocene] derivatives (0.05 mmol) were dissolved in a mixture of CH_3CN/CH_2Cl_2 (1:5; 3 mL), and the corresponding metal salt (0.05 mmol) was added. The original orange solution became immediately red for the copper salt and stayed orange for the others. The reaction mixture was stirred for 4 h at RT, and then the solvent was evaporated to dryness. After drying, a red-orange solid was obtained quantitatively. This solid was normally used without further purification for analysis.

[Cu_2 $\mathbf{1}_2$**](PF_6)$_2$ (C1).** ^{1}H NMR (400 MHz, CD_3CN, *δ*): 7.95 (m, 4H, H(3′)); 7.83 (m, 8H, H(3), H(4′)); 7.72 (m, 4H, H(4)); 7.42 (br, 4H, H(5′)); 5.55 (br, 4H, H(α)); 5.25 (br, 4H, H(α)); 4.60 (br, 8H, H(*β*)); 2.95 (m, 8H, H(7)); 2.72 (m, 4H, H(10)); 2.48 (m, 4H, H(9_b)); 2.31 (m, 4H, H(8)); 1.31 (s, 12H, H(12)); 1.05 (d, 4H, H(9_a), $^2J_{9a,9b}$ = 9.0 Hz); 0.23 (s, 12H, H(13)). ESI-MS: *m*/*z* = 1637.43 ([Cu_2**1**$_2$$PF_6$]$^+$, 10%), 745.22 ([$Cu_2$**1**$_2$]$^{2+}$, 100%). UV−vis ($CH_2Cl_2$) [*λ* (*ϵ*)]: 440 nm (2.6 × 10^3); 327 nm (3.5 × 10^4); 273 nm (2.5 × 10^4). CD (CH_2Cl_2) [*λ* (Δ*ϵ*)]: 331 nm (+22); 307 nm (−25). X-ray crystal structure determination: A suitable crystal of **C1**·5.25CH_2Cl_2 was obtained as a red crystal by slow diffusion of toluene in a dichloromethane solution. The crystal was mounted on a Stoe imaging plate diffractometer system (Stoe, 2000 no. 11) equipped with a one-circle *φ* goniometer and a graphite-monochromator. Data collection was performed at −120 °C/153 K using Mo Kα radiation (*λ* = 0.710 73 Å). A total of 200 exposures (3 min/exposure) were obtained at an image plate distance of 70 mm with 0 < *φ* < 180° and with the crystal oscillating through 1° in *φ*. The resolution was D_{min}−D_{max} 12.45−0.81 Å. The compound was found in a monoclinic cell (*C*2). The molecular formula of the compound was {[$Cu_2Fe_2(C_{21}H_{21}N_2)_4$]($PF_6$)$_4$($C_2H_2Cl_2$)$_{5.25}$}. The SQUEEZE instruction in PLATON99[24] was used to calculate the potential solvent accessible area in the unit cell; 4419 Å^3 were calculated containing about 893 electrons. Therefore, 21 dichloromethane (882 electrons) molecules/unit cell were included in all further calculations. The structure was solved by direct methods using the program SHELXS-97 (Sheldrick, 1990, no. 12) and refined by full-matrix least squares on F^2 with SHELXL-97.[Sheldrick, 1999, no. 13] The hydrogen atoms were included in calculated positions and treated as riding atoms using SHELXL-97 default parameters. All non-hydrogen atoms were refined anisotropically. An empirical absorption correction was applied using DIFABS (PLATON99,[24] T_{min} = 0.215, T_{max} = 0.681).

[Cu_2 $\mathbf{2}_2$**](PF_6)$_2$ (C2).** ^{1}H NMR (400 MHz, CD_3CN, *δ*): 7.95 (m, 4H, H(3′)); 7.83 (m, 8H, H(3), H(4′)); 7.72 (m, 4H, H(4)); 7.42 (br, 4H, H(5′)); 5.55 (br, 4H, H(α)); 5.25 (br, 4H, H(α)); 4.60 (br, 8H, H(*β*)); 2.95 (m, 8H, H(7)); 2.72 (m, 4H, H(10)); 2.48 (m, 4H, H(9_b)); 2.31 (m, 4H, H(8)); 1.31 (s, 12H, H(12)); 1.05 (d, 4H, H(9_a), $^2J_{9a,9b}$ = 9.0 Hz); 0.23 (s, 12H, H(13)). ESI-MS: *m*/*z* = 1637.43 ([Cu_2**2**$_2$$PF_6$]$^+$, 10%), 745.22 ([$Cu_2$**2**$_2$]$^{2+}$, 100%). UV−vis ($CH_2Cl_2$) [*λ* (*ϵ*)]: 440 nm (2.6 × 10^3); 327 nm (3.5 × 10^4); 273 nm (2.5 × 10^4). CD (CH_2Cl_2) [*λ* (Δ*ϵ*)]: 331 nm (−22); 308 nm (+26). X-ray crystal structure determination: A suitable crystal of **C2**·8.5CH_2Cl_2 was obtained as a red crystal. The crystal was mounted on a Stoe Mark II imaging plate diffraction system (Stoe, 2000 no. 11) equipped with a graphite monochromator. Data collection was performed at −120 °C/153 K using Mo Kα radiation (*λ* = 0.710 73 Å). A total of 219 exposures (10 min/exposure) were obtained at an image plate distance of 140 mm with 180 frames *φ* = 0° and 0 < *φ* < 180°, with 39 frames *φ* = 90° and 0 < *φ* < 90°, and with the crystal oscillating through 1° in *φ*. The resolution was D_{min}−D_{max} 24.88−0.83 Å. The structure was solved by direct methods using the program SHELXS-97 (Sheldrick, 1990, no. 12) and refined by full-matrix least squares on F^2 with SHELXL-97 (Sheldrick, 1999, no. 13). The hydrogen atoms were included in calculated positions and treated as riding atoms using SHELXL-97 default parameters. This compound crystallized in the orthor-

(24) Spek, A. L. *Acta Crystallogr*. **1990**, *A46*, C34.

hombic noncentrosymmetric space group $P2_12_12_1$. It was a racemic twin, and the final refined Flack *x* parameter was 0.16(2). The SQUEEZE instruction in PLATON99[24] was used to calculate the potential solvent-accessible area in the unit cell; 3688 Å^3 were calculated containing ca. 1430 electrons. This was estimated to be equivalent to 34 dichloromethane (1428 electrons) molecules/unit cell, which were taken into consideration in all further calculations. The molecular formula is therefore $\{[Cu_2Fe_2(C_{21}H_{21}N_2)_4](PF_6)_2(CH_2Cl_2)_{8.5}\}$.

$[Ag_2\mathbf{1}_2](PF_6)_2$ (C3). ^{1}H NMR (400 MHz, CD_3CN, δ): 8.12−7.45 (br, 20H, H(3′), H(3), H(4′), H(4), H(5′)); 5.45 (br, 8H, H(Fc)); 4.85−4.55 (br, 8H, H(Fc)); 2.95−2.45 (br, 20H, H(7), H(10), H(9_b), H(8)); 1.32 (s, 12H, H(12)); 0.90 (br, 4H, H(9_a)); 0.45 (s, 12H, H(13)). ESI-MS: m/z = 791.24 ($[Ag_2\mathbf{1}_2]^{2+}$, 100%). UV−vis: (CH_2Cl_2) [λ (ϵ)]: 476 nm (1.3×10^3); 310 nm (4.8×10^4); 282 nm (4.8×10^4). CD (CH_2Cl_2) [λ ($\Delta\epsilon$)]: 329 nm (−101); 303 nm (+127). X-ray crystal structure determination: A suitable crystal of **C3**·$3CH_2Cl_2$ was obtained as a red crystal using ClO_4^- counterion. The crystal was mounted on a Stoe Mark II imaging plate diffractometer system (Stoe, 2000 no. 11) equipped with a graphite monochromator. Data collection was performed at −120 °C using Mo Kα radiation (λ = 0.710 73 Å). A total of 85 exposures (12 min/exposure) were obtained at an image plate distance of 140 mm with 85 frames $\varphi = 90°$ and $15 < \varphi < 160.5°$ and with the crystal oscillating through 1.5° in ϕ. The resolution was $D_{min}-D_{max}$ 24.88−0.83 Å. This compound was found in the noncentrosymmetric monoclinic space group $P2_1$ [Flack parameter $x = -0.05(7)$]. The molecular formula of this compound is $\{[Ag_2Fe_2(C_{22}H_{21}N_2)_4](ClO_4)_2(CH_2Cl_2)_3\}$. The SQUEEZE instruction in PLATON99[24] was used to calculate the potential solvent-accessible area in the unit cell; 1562 Å^3 were calculated containing about 246 electrons. Therefore, 6 dichloromethane (252 electrons) molecules/unit cell were included in all further calculations. The structure was solved by direct methods using the program SHELXS-97 (Sheldrick, 1990, no. 12) and refined by full-matrix least squares on F^2 with SHELXL-97 (Sheldrick, 1999, no. 13). As a result of the weakly diffracting crystal, only the metal atoms were refined anisotropically and no hydrogen atom were included; the final R-value is high with 0.11, and high standard uncertainties were found for distances and angles.

$[Zn_2L15_2](PF_6)_4$ (C4). ^{1}H NMR (400 MHz, CD_3CN, δ): 8.41 (br, 4H, H(3′)); 8.32 (br, 8H, H(3), H(4′)); 8.25 (br, 4H, H(4)); 7.90 (br, 4H, H(5′)); 5.05 (br, 16H, H(Fc)); 3.00 (br, 8H, H(7)); 2.75 (m, 4H, H(10)); 2.50−2.30 (m, 8H, H(9_b), H(8)); 1.40 (s, 12H, H(12)); 1.1 (d, 4H, H(9_a), $^2J_{9a,9b}$ = 9.5 Hz); 0.3 (s, 12H, H(13)). ESI-MS: m/z = 893.20 ($[Zn_2L15_2(PF_6)_2]^+$, 100%). UV−vis (CH_2Cl_2) [λ (ϵ)]: 475 nm (2.8×10^3); 335 nm (6.2×10^4); 290 nm (4.1×10^4). CD (CH_2Cl_2) [λ ($\Delta\epsilon$)]: 354 nm (+102); 325 nm (−130).

$[Cu_2\mathbf{3}_2](PF_6)_2$ (C5). ^{1}H NMR (400 MHz, CD_3CN, δ): 8.25 (br, 4H, H(3)); 8.05−7.82 (br, 12H, H(3′), H(4′), H(6)); 7.80−7.62 (br, 4H, H(5′)); 5.41 (br, 4H, H(Fc)); 5.1 (br, 4H, H(Fc)); 4.62 (br, 4H, H(Fc)); 4.48 (br, 4H,H(Fc)); 3.12 (br, 8H, H(7)); 2.98 (br, 4H, H(10)); 2.65 (br, 4H, H(9_b)); 2.5 (br, 4H, H(8)); 1.35 (s, 12H, H(12)); 1.05 (br, 4H, H(9_a)); 0.55 (s, 12H, H(13)). ESI-MS: m/z = 1637.44 ($[Cu_2\mathbf{3}_2PF_6]^+$, 2%), 745.23 ($[Cu_2\mathbf{3}_2]^{2+}$, 100%). UV−vis ($CHCl_3$) [λ (ϵ)]: 437 nm (5.2×10^3); 308 nm (5.1×10^4); 279 nm (6.9×10^4). CD ($CHCl_3$) [λ ($\Delta\epsilon$)]: 326 nm (+43); 305 nm (−38). X-ray crystal structure determination: Suitable crystals of **C5**·3toluene·0.2dichloromethane solvate were obtained as red blocks by slow diffusion of toluene in a dichloromethane solution. The intensity data were collected at 153 K on a Stoe image plate diffraction system (Stoe, 2000 no. 11) using Mo Kα graphite-monochromated radiation: image plate distance, 70 mm; ϕ oscillation scans, 0−200°; step $\Delta\phi = 1.0°$; 2θ range, 3.27−52.1°; $D_{max}-D_{min}$ = 12.45−0.81 Å. The structure was solved by direct methods using the program SHELXS-97 (Sheldrick, 1990, no. 12]. The refinement and all further calculations were carried out using SHELXL-97 (Sheldrick, 1999, no. 13). The H atoms were included in calculated positions and treated as riding atoms using SHELXL default parameters. The non-H atoms were refined anisotropically, using weighted full-matrix least squares on F^2. One of the PF_6 anions is disordered, and one of the dichloromethane solvent molecules of crystallization is also disordered; the hydrogen atoms were not included for the latter calculations.

$[Cu_2\mathbf{1a}_2](PF_6)_2$ (C6). ^{1}H NMR (400 MHz, $CDCl_3$, δ): 8.40 (d, 4H, H(3′), $^3J_{3',4'}$ = 8 Hz); 8.30 (d, 4H, H(3), $^3J_{3,4}$ = 8 Hz); 8.16 (m, 4H, H(4′)); 8.02 (m, 4H, H(4)); 7.61 (d, 4H, H(5′), $^3J_{5',4'}$ = 8 Hz); 5.95−5.60 (br, 8H, H(Fc)); 4.90−4.80 (br, 8H, H(Fc)); 2.83 (m, 4H, H(7)); 2.43 (m, 8H, H(10), H(9_b)); 1.82 (m, 4H, H(8)); 1.26 (s, 12H, H(12)); 1.08 (d, 4H, H(9_a), $^2J_{9a,9b}$ = 9.9 Hz); 0.91 (d, 12H, H(14), $^3J_{14,7}$ = 7.0 Hz); 0.02 (s, 12H, H(13)). ESI-MS: m/z = 1079.02 ($[Cu_2\mathbf{1a}_2PF_6]^+$, 5%), 773.24 ($[Cu_2\mathbf{1a}_2]^{2+}$, 100%). UV−vis ($CHCl_3$) [$\lambda$ (ϵ)]: 319 nm (4.6×10^4), 271 nm (5.2×10^4). CD ($CHCl_3$) [λ ($\Delta\epsilon$)]: 330 nm (+69); 303 nm (−30).

$[Cu_2\mathbf{1b}_2](PF_6)_2$ (C7). ^{1}H NMR (400 MHz, acetone-d_6, δ): 8.45 (br m, 8H, H(3′), H(3)); 8.07 (m, 4H, H(4′)); 7.90 (m, 4H, H(4)); 7.72 (m, 4H, H(5′)); 6.95 (br m, 20H, H(15), H(16), H(17)); 5.90−5.72 (br, 8H, H(Fc)); 4.95−4.55 (br, 8H, H(Fc)); 3.62 (m, 4H, H(14_b)); 2.80−2.25 (br m, 20H, H(7)), H(10), H(9_b), H(8), H(14_a)); 1.18 (s, 12H, H(12); 1.09 (br, 4H, H(9_a)); 0.02 (s, 12H, H(13)). ESI-MS: m/z = 1997.66 ($[Cu_2\mathbf{1b}_2PF_6]^+$, 2%), 925.32 ($[Cu_2\mathbf{1b}_2]^{2+}$, 100%). UV−vis ($CHCl_3$) [$\lambda$ (ϵ)]: 317 nm (5.8×10^4); 281 nm (7.0×10^4). CD ($CHCl_3$) [λ ($\Delta\epsilon$)]: 322 nm (+257); 302 nm (−127).

$[Cu_2\mathbf{1c}_2](PF_6)_2$ (C8). ^{1}H NMR (400 MHz, $CDCl_3$, δ): 8.35 (m, 4H, H(3′)); 8.30 (m, 4H, H(3)); 8.15 (m, 4H, H(4′)); 7.92 (m, 4H, H(4)); 7.61 (m, 4H, H(5′)); 5.40 (m, 4H, H(Fc)); 4.85 (m, 4H, H(Fc)); 4.62 (m, 8H, H(Fc)); 3.05 (m, 4H, H(7)); 2.95 (m, 4H, H(14)); 2.18 (m, 8H, H(10)); 2.5 (m, 4H, H(9_b)); 2.30 (m, 4H, H(8)); 1.22 (s, 12H, H(12)); 1.18 (br d, 4H, H(9_a)); 0.40 (m, 12H, H(15)); 0.15 (m, 12H, H(16)); 0.0 (s, 12H, H(13)). ESI-MS: m/z = 829.30 ($[Cu_2\mathbf{1c}_2]^{2+}$, 100%). UV−vis: ($CHCl_3$) [λ (ϵ)]: 316 nm (5.4×10^4); 280 nm (6.7×10^4). CD ($CHCl_3$) [λ ($\Delta\epsilon$)]: 330 nm (+198); 303 nm (−115).

Acknowledgment. This research was performed with the financial support of the Swiss National Science Foundation.

Supporting Information Available: Crystallographic data in CIF format. This material is available free of charge via the Internet at http://pubs.acs.org.

IC049913A